PROCEEDINGS OF SCIENCE

Measuring the Astrophysical $\nu : \bar{\nu}$ Ratio with IceCube

The IceCube Collaboration

(a complete list of authors can be found at the end of the proceedings)

E-mail: bskrzypek@lbl.gov, srklein@lbl.gov

Recent measurements of astrophysical neutrinos have expanded our understanding of their nature and origin. However, very little is still known about the astrophysical $\nu/\bar{\nu}$ ratio. The only prior measurement is the recent, single Glashow event seen by IceCube. Understanding the astrophysical $\nu/\bar{\nu}$ ratio has a bearing on multiple questions, including the astrophysical spectral shape and neutrino production mechanisms. This analysis uses a new approach to measuring the astrophysical muon $\nu/\bar{\nu}$ ratio at various energies. It uses inelasticity, the fraction of the initial neutrino energy carried away by the hadronic shower. Inelasticity probes the $\nu/\bar{\nu}$ ratio due to the fact that at energies below roughly 100 TeV, valence quarks dominate in deep inelastic scattering interactions, leading to different neutrino and antineutrino inelasticities and cross-sections. We use 10.3 years of IceCube data consisting of starting tracks at energies between 1 TeV and 1 PeV with a self-veto selection that enhances astrophysical event purity in the down-going direction. Based on this sample and analysis method, we present the first measurement of the astrophysical $\nu/\bar{\nu}$ ratio at sub-PeV energies.

Corresponding authors: Barbara Skrzypek[1,2*], Spencer Klein[1,2]

[1] *University of California, Berkeley*

[2] *Lawrence Berkeley National Laboratory*

[*] Presenter

39th International Cosmic Ray Conference (ICRC2025)
15–24 July 2025
Geneva, Switzerland

ICRC 2025
The Astroparticle Physics Conference
Geneva July 15-24, 2025

© Copyright owned by the author(s) under the terms of the Creative Commons Attribution-NonCommercial-NoDerivatives 4.0 International License (CC BY-NC-ND 4.0).

PoS(ICRC2025)1181

1. Introduction

Despite multiple measurements of the high-energy astrophysical neutrino spectrum, the astrophysical $\nu/\bar{\nu}$ ratio across all three flavors remains largely unconstrained. The astrophysical $\nu/\bar{\nu}$ ratio has a bearing on multiple important questions, including the astrophysical spectral shape, production mechanisms at the source, and the types of environments and circumstances from which astrophysical neutrinos originate, such as photon density, cosmic-ray mass compositions, and magnetic field strengths. For example, pp interactions, which are expected to be the dominant mechanism in star-forming galaxies, result in equal parts neutrinos and antineutrinos for both electron and muon flavors through $pp \rightarrow \pi^{\pm} \rightarrow \nu_e + \bar{\nu}_e + 2\nu_\mu + 2\bar{\nu}_\mu$. However, in the muon-damped scenario such as in the presence of a strong magnetic field, only muon-neutrinos result. On the other hand, $p\gamma$ interactions, which produce neutrinos through $p\gamma \rightarrow \pi^{+} \rightarrow \nu_e + \nu_\mu + \bar{\nu}_\mu$, result in an electron-neutrino and equal parts muon neutrino and antineutrino. The $\nu/\bar{\nu}$ ratios are different between the two flavors. In the corresponding muon-damped scenario, in which $p\gamma \rightarrow \pi^{+} \rightarrow \nu_\mu$, only one muon-neutrino results.

Few probes are sensitivite to the astrophysical $\nu/\bar{\nu}$ ratio. One such example is the detection of an electron-antineutrino undergoing Glashow resonance [1]. This was detected by IceCube at 6 PeV with a significance of 5σ. However, this observable only gives us access to the electron-neutrino $\nu/\bar{\nu}$ component at very high energies.

Inelasticity is another probe that offers sensitivity to other flavor components and over a wider energy range. In deep inelastic scattering (DIS) interactions, inelasticity is defined to be the fraction of the initial neutrino energy that gets carried away by the hadronic shower [2]. At Cherenkov detectors, it is sensitive to charged current interactions with muons. Due to the fact that valence quarks, which dominate at lower energies, interact at different rates with neutrinos and antineutrinos, the corresponding cross-sections differ, leading to different inelasticities, particularly at lower energies. Previous IceCube measurements of inelasticity were used to test the atmospheric $\nu : \bar{\nu}$ ratio and neutrino charm quark production [3], and a recent measurement extended our understanding of inelasticity in neutrino DIS to below 560 GeV [4].

2. Analysis

In DIS, the charged-current cross-section for neutrinos and anti-neutrinos is given by [5]

$$\frac{d^2\sigma^{\nu,\bar{\nu}}}{dxdy} = \frac{G_F^2 M_N E_\nu}{\pi(1+Q^2/M_W^2)^2}\left[\frac{y^2}{2}2xF_1(x,Q^2) + \left(1 - y - \frac{M_N xy}{2E_\nu}\right)F_2(x,Q^2) \pm y\left(1-\frac{y}{2}\right)xF_3(x,Q^2)\right], \tag{1}$$

where the +(−) sign refers to neutrino (anti-neutrino) interactions, $G_F = 1.17 \times 10^{-5}$ GeV^{-2}, M_N is the nucleon mass, and the kinematic variables are defined as

$$x = Q^2/2M_N E_\nu y, \tag{2}$$

$$y = E_{\rm had}/E_\nu = (E_\nu - E_\ell)/E_\nu, \tag{3}$$

$$Q^2 = (p_\nu - k_\ell)^2 = -m_\ell^2 + 2E_\nu(E_\ell - p_\ell \cos\theta_\ell). \tag{4}$$

The factors $F_i(x, Q^2)$ are the dimensionless nucleon structure functions. Under the quark-parton model, these can be expressed in terms of the corresponding quark parton distribution functions,

PoS(ICRC2025)1181

which depend on the target and type of interaction involved. In the case of $\bar{\nu}p \to \mu^+ X$ scattering, the *leading order* structure functions can be expressed as a sum over the active quark parton distribution functions:

$$F_2^{W^-}(x, Q^2) = 2x(u + c + b + \bar{d} + \bar{s} + \bar{t}), \tag{5}$$

$$xF_3^{W^-}(x, Q^2) = 2x(u + c + b - \bar{d} - \bar{s} - \bar{t}). \tag{6}$$

The structure functions corresponding to $\nu n \to \mu^- X$ scattering are obtained through the interchange $u \leftrightarrow d$. The third structure function, $xF_1(x, Q^2)$, is related to F_2 via a longitudinal structure function that quantifies the ratio of scattering off of longitudinally and transversely polarized W bosons. In the quark-parton model, which is valid at leading-order, this simplifies to $2xF_1 = F_2$ for both neutral- and charged-current interactions. Applying the leading order structure functions and ignoring terms proportional to $1/E_\nu$, we obtain the following for neutrinos and anti-neutrinos:

$$\frac{d^2\sigma^{\bar{\nu}}}{dxdy} = \frac{G_F^2 M_N E_\nu}{\pi(1 + Q^2/M_W^2)^2}\left[2x\left(\bar{d} + \bar{s} + \bar{t} + (1 - y)^2(u + c + b)\right)\right], \tag{7}$$

$$\frac{d^2\sigma^{\nu}}{dxdy} = \frac{G_F^2 M_N E_\nu}{\pi(1 + Q^2/M_W^2)^2}\left[2x\left(d + s + t + (1 - y)^2(\bar{u} + \bar{c} + \bar{b})\right)\right]. \tag{8}$$

From the double-differential cross-section, we obtain inelasticity distributions by integrating over y and normalizing by the total cross-section:

$$\frac{dp_\nu}{dy} = \frac{1}{\sigma_\nu}\int_0^1 dx \frac{d^2\sigma_\nu}{dxdy}, \quad \frac{dp_{\bar{\nu}}}{dy} = \frac{1}{\sigma_{\bar{\nu}}}\int_0^1 dx \frac{d^2\sigma_{\bar{\nu}}}{dxdy}. \tag{9}$$

To compute the probability distribution function corresponding to a scenario in which the ratio $\nu/(\nu + \bar{\nu}) = r$, we combine the individual probability distribution functions in the following way:

$$\frac{dp}{dy} = r\frac{dp_\nu}{dy} + (1 - r)\frac{dp_{\bar{\nu}}}{dy}. \tag{10}$$

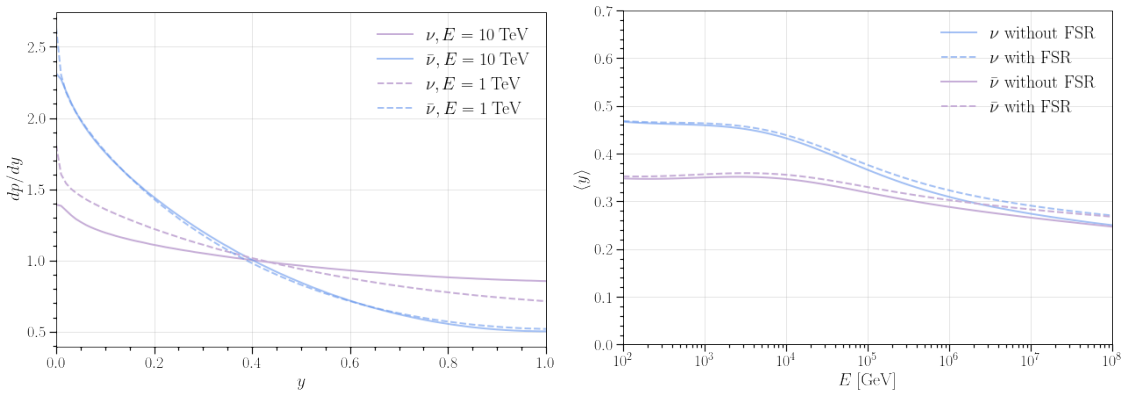


Figure 1: Left: The inelasticity probability distribution functions for neutrinos and antineutrinos at two different energies. Right: The mean inelasticity $\langle y \rangle \equiv \int dy y(dp/dy)$ as a function of energy. The dashed lines correspond to the mean inelasticity including a correction for final state radiation (FSR) [6].

PoS(ICRC2025)1181

We use a recent set of leading-order quark parton distribution functions (PDFs). These are given by CTLO18A [7] and documented in `LHAPDF` [8]. At lower energies, the PDFs of the valence quarks dominate, leading to different quark and antiquark distributions. At higher energies, sea quarks begin to play a bigger role, and thus the difference between neutrino and antineutrino interactions becomes smaller. The resulting inelasticity PDFs, defined as $\frac{1}{\sigma}\frac{d\sigma}{dy}$, differ at different energies and varying $\nu : \bar{\nu}$ ratios. An all-neutrino spectrum prefers larger inelasticities while an all-antineutrino spectrum prefers smaller inelasticities.

To account for nuclear effects in DIS interactions in ice, we use nuclear PDFs for ^{16}O, given by EPPS21 and CT18A. We then combine the $\nu -^{16}$ O cross-section built out of these PDFs with the $\bar{\nu} - p$ cross-section, obtained using the nuleon PDFs described above. This results in the cross-section for an H_2O target.

2.1 Data Sample

The IceCube Neutrino Observatory is a cubic-kilometer Cherenkov detector located at the South Pole, 1.5 km below the surface of the ice [9]. Strings running from below the ice to the computing lab consist of a total of 5160 digital optical modules (DOMs) that detect Cherenkov radiation from charged particles using photomultiplier tubes.

In order to measure the astrophysical $\nu/\bar{\nu}$ ratio, we use the Enhanced Starting Tracks Event Selection (ESTES) from the IceCube neutrino observatory, which has a number of benefits. As a starting events sample, it offers comparatively good energy resolution and allows us to reconstruct inelasticity, while tracks provide good angular resolution. Additionally, to remove the atmospheric muon background, ESTES makes use of a dynamic self-veto in the southern sky which reduces background while retaining a significant number of astrophysical signal events. We use the most recent 10.3 year sample with the dynamic self-veto. Our energies of interest range from 1 TeV to 10 PeV, and we probe neutrino directions covering the entire sky. We also use visible inelasticity [3], which is defined as the fraction of the total energy reconstructed as a cascade.

To compute the direction of an event, a series of increasingly complex reconstruction algorithms are used, where the seed for each subsequent algorithm is the reconstruction direction of the previous algorithm. This includes `Millipede` [10], which uses information from all available DOMs and divides track into segments, fitting an energy-loss for each segment, so as to account for the stochastic energy loss of muons.

We use an energy reconstruction based on a random forest algorithm [11]. This reconstructs the estimated initial hadronic and leptonic energies based on deposited track and cascade energies. From there, we calculate inelasticity by dividing the reconstructed hadronic energy by the sum of hadronic and track energies.

2.2 Systematics

We use a combination of physics and detector systematics to properly model uncertainties. These systematics are interpolated over reconstructed energy, zenith angle, and inelasticity. A summary of the systematics along with priors and allowed ranges is given in Table 1.

The detector systematics that we use to parameterize uncertainties in the IceCube detector include: DOM efficiency, or a scaling factor describing the sensitivity of the individual digital optical

PoS(ICRC2025)1181

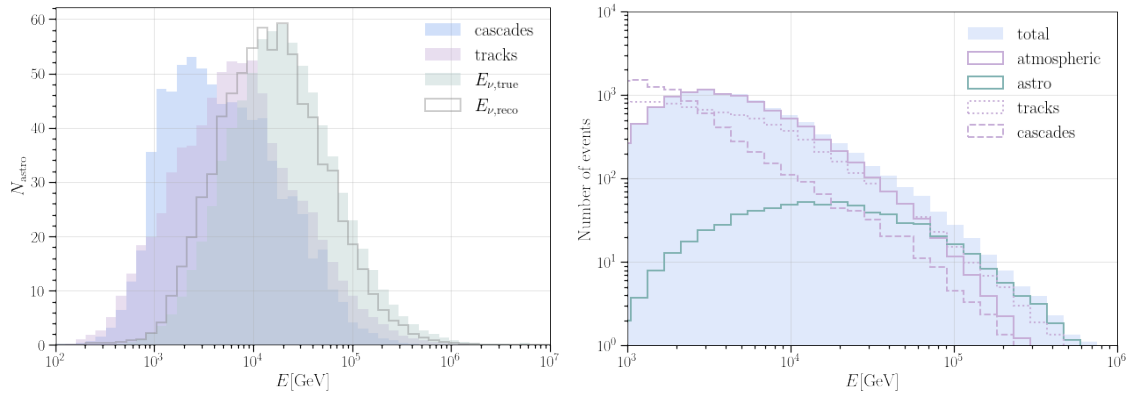


Figure 2: The reconstructed neutrino energy event distributions for different components of the neutrino spectrum. Astrophysical events are shown on the left, and a comparison of astrophysical, atmospheric, and total events is shown on the right.

modules in the ice [12]; two hole ice parameters p_0 and p_1 based on an angular response function [13] that models effects from ice impurities caused by the columns of refrozen ice surrounding the DOMs [14, 15]; and scattering and absorption coefficients [16] used in simulations to account for depth-dependent uncertainties in photon propagation in the bulk ice [17, 18] .

We model the atmospheric neutrino flux uncertainty according to the Global Spline Fit (GSF) parameters for the cosmic ray spectrum as well as the Data-Driven Model (DDM) describing the hadronic interaction uncertainties. Together, these are known as the Daemonflux parameters [19]. Compared to other fits to data, such as the Barr parameterization [20], the predictions and corresponding uncertainties are very different. The reason they are so large in Barr is because they assume a 40% uncertainty in $K^{\pm}$ production at high energies, whereas Daemonflux uses a data-driven approach. There are also slight differences in the choice of primary flux, and differences in kaon abundance can result from different fits.

We assume an astrophysical single power law flux as shown here:

$$\phi_{\mathrm{astro}}^{\mathrm{baseline}}(E) = \phi_0 \left(\frac{E}{100\ \mathrm{TeV}}\right)^{-\gamma}, \quad \phi_0 = 1.68 \times 10^{-18}\ \mathrm{GeV}^{-1}\mathrm{cm}^{-2}\mathrm{s}^{-1}\mathrm{sr}^{1},\ \gamma = 2.58. \tag{11}$$

2.3 Fit Procedure

For each point in the physics parameter space of $r_{\mathrm{astro}} \equiv \left(\nu/(\nu+\bar{\nu})\right)_{\mathrm{astro}}$ and $r_{\mathrm{atm}} \equiv \left(\frac{\nu}{\nu+\bar{\nu}}\right) \Big/ \left(\frac{\nu}{\nu+\bar{\nu}}\right)_{\mathrm{nominal}}$, we generate a predicted event distribution. We then perform the fit using a binned Poisson likelihood method, where the test statistic is

$$-2\ln\Lambda = \sum_i \left(\mu_i(\theta) - n_i + n_i \ln\left(\frac{n_i}{\mu_i(\theta)}\right)\right) + \sum_j \frac{(\theta_j - \theta_j^*)^2}{\sigma_j^2}, \tag{12}$$

where $\mu_i(\theta)$ is the expected event count per bin and n_i is the observed event count. The second term is a Gaussian penalty for systematic parameter θ_j with mean θ_j^* and standard deviation σ_j. We minimize this over our set of physics and systematic parameters, denoted by θ, using `Minuit` [21].

PoS(ICRC2025)1181

Systematic	Central	Prior (1σ)	Range	Implementation
Detector Parameters				
DOM efficiency	1.27	±10%	[1.234, 1.346]	Spline over 6 knots
Hole Ice p_0	-0.3	±0.5	[-2,1]	Spline over 6 knots
Hole Ice p_1	-0.1	±0.5	[-0.2,0.2]	Spline over 6 knots
Scattering	1.05	±0.05	[0.8,1.2]	Spline over 6 knots
Absorption	1.00	±0.05	[0.8,1.2]	Spline over 6 knots
Conventional Flux Parameters				
$K^{\pm}_{158G}$, $\pi^{\pm}_{20T}$, $K^{\pm}_{2P}$, $\pi^{\pm}_{2P}$, p_{2P}, n_{2P}	0.0	±1.0	[-2, 2]	Spline over 9 knots
GSF_{1-6}	0.0	±1.0	[-4, 4]	Spline over 9 knots
High-energy Flux Parameters				
Normalization	1.68	±0.36	[0,3]	Flux rescaling
$\Delta\gamma_1$, tilt from -2.5	0.0	±0.36	[-2,2]	Flux reweighting

Table 1: List of systematic parameters considered in this analysis along with their central values, priors, allowed ranges, and implementations. The atmospheric systematics include the Data-Driven Model (DDM) as well as the cosmic-ray Global Spline Fit (GSF) parameters [19].

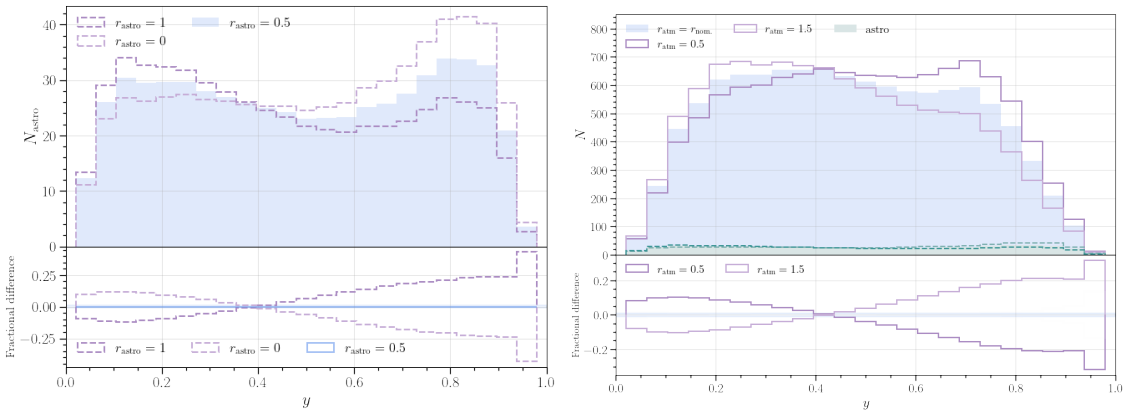


Figure 3: Left: The inelasticity distributions of astrophysical events under different assumptions of r_{astro}. The bottom panel shows the fractional difference between each scenario and the nominal scenario, in which $r_{\text{astro}} = 0.5$. Right: The total inelasticity distributions under different assumptions of r_{atm}. The bottom panel shows the fractional difference between each of these scenarios and the nominal model, in which $r_{\text{atm}} = 1$.

3. Sensitivity

Figure 4 shows the Asimov sensitivities that we obtained by injecting a nominal model that assumes $r_{\text{astro}} = 0.5$ and $r_{\text{atm}} = 1$ and performing a fit over a 25×25 grid over $0 \leq r_{\text{astro}} \leq 1$ and $0.5 \leq r_{\text{atm}} \leq 1.5$.

The projected sensitivity predicts a closed contour at 1σ with 10.3 years of data.

PoS(ICRC2025)1181

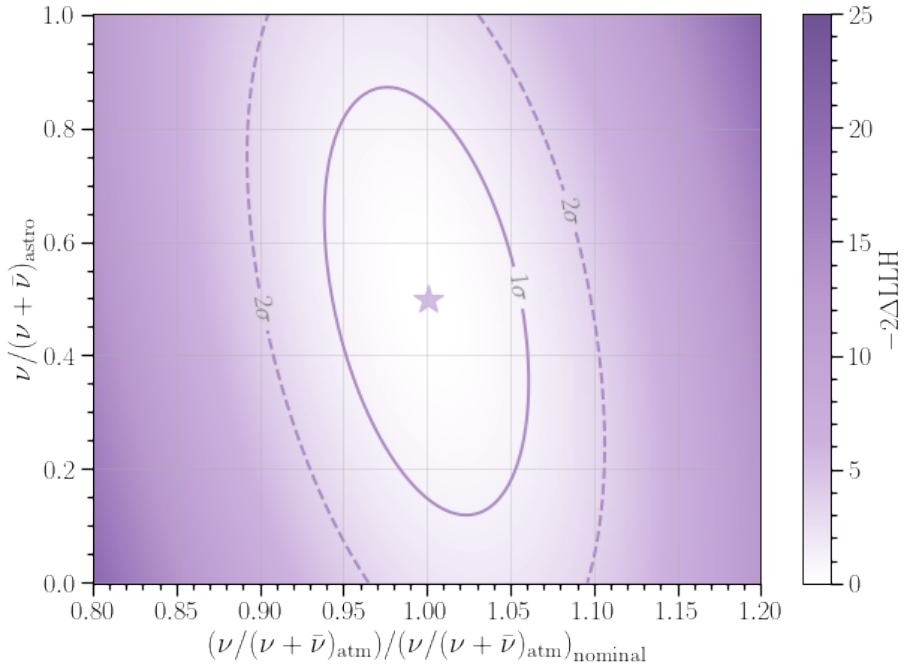


Figure 4: The Asimov sensitivity obtained when injecting $r_{\text{astro}} = 0.5$ and $r_{\text{atm}} = 1$.

4. Conclusion

The results presented in this proceeding consist of the first measurement of the astrophysical $\nu : \bar{\nu}$ ratio ever, outside of the single Glashow event detected by IceCube. This result will shed light on numerous questions about the astrophysical neutrino flux, including which production mechanisms that could be involved.

References

[1] R. Abbasi *et al.*, *Nature* **591** no. 7849, (Mar., 2021) 220–224.

[2] S. R. Klein, *Probing high-energy interactions of atmospheric and astrophysical neutrinos*. 2020. arXiv:1906.02221 [astro-ph.HE].

[3] M. Aartsen *et al.*, *Physical Review D* **99** no. 3, (Feb., 2019) .

[4] M. Aartsen *et al.*, *Physical Review D* **111** no. 11, (June, 2025) .

[5] J. A. Formaggio and G. P. Zeller, *Reviews of Modern Physics* **84** no. 3, (Sept., 2012) 1307–1341.

[6] R. Plestid and B. Zhou, "Final state radiation from high and ultrahigh energy neutrino interactions," 2024. https://arxiv.org/abs/2403.07984.

[7] T.-J. Hou, J. Gao, T. Hobbs, K. Xie, S. Dulat, M. Guzzi, J. Huston, P. Nadolsky, J. Pumplin, C. Schmidt, I. Sitiwaldi, D. Stump, and C.-P. Yuan, *Physical Review D* **103** no. 1, (2021) .

PoS(ICRC2025)1181

[8] A. Buckley, J. Ferrando, S. Lloyd, K. Nordström, B. Page, M. Rüfenacht, M. Schönherr, and G. Watt, *The European Physical Journal C* **75** no. 3, (Mar., 2015) .

[9] M. Aartsen *et al.*, *Journal of Instrumentation* **12** no. 03, (Mar., 2017) P03012–P03012.

[10] M. Aartsen *et al.*, *Journal of Instrumentation* **9** no. 03, (Mar., 2014) P03009–P03009.

[11] J. Breiman, *Machine Learning* **45** (2001) 5–32.

[12] R. Abbasi *et al.*, *Nuclear Instruments and Methods in Physics Research Section A: Accelerators, Spectrometers, Detectors and Associated Equipment* **618** no. 1–3, (June, 2010) 139–152.

[13] R. Abbasi *et al.*, *Phys. Rev. D* **108** (Jul, 2023) 012014.

[14] **IceCube** Collaboration, M. Rongen, *EPJ Web Conf.* **116** (2016) 06011.

[15] S. Fiedlschuster, "The effect of hole ice on the propagation and detection of light in icecube," 2019. https://arxiv.org/abs/1904.08422.

[16] Askebjer *et al.*, *Applied Optics* **36** no. 18, (June, 1997) 4168.

[17] M. Ackermann *et al.*, *J. Geophys. Res.* **111** no. D13, (2006) D13203.

[18] *Nuclear Instruments and Methods in Physics Research Section A: Accelerators, Spectrometers, Detectors and Associated Equipment* **711** (May, 2013) 73–89.

[19] J. P. Yañez and A. Fedynitch, *Physical Review D* **107** no. 12, (June, 2023) .

[20] G. D. Barr, S. Robbins, T. K. Gaisser, and T. Stanev, *Physical Review D* **74** no. 9, (Nov., 2006) .

[21] F. James and M. Roos, *Comput. Phys. Commun.* **10** (1975) 343–367.

PoS(ICRC2025)1181

Full Author List: IceCube Collaboration

R. Abbasi[16], M. Ackermann[63], J. Adams[17], S. K. Agarwalla[39, a], J. A. Aguilar[10], M. Ahlers[21], J.M. Alameddine[22], S. Ali[35], N. M. Amin[43], K. Andeen[41], C. Argüelles[13], Y. Ashida[52], S. Athanasiadou[63], S. N. Axani[43], R. Babu[23], X. Bai[49], J. Baines-Holmes[39], A. Balagopal V.[39, 43], S. W. Barwick[29], S. Bash[26], V. Basu[52], R. Bay[6], J. J. Beatty[19, 20], J. Becker Tjus[9, b], P. Behrens[1], J. Beise[61], C. Bellenghi[26], B. Benkel[63], S. BenZvi[51], D. Berley[18], E. Bernardini[47, c], D. Z. Besson[35], E. Blaufuss[18], L. Bloom[58], S. Blot[63], I. Bodo[39], F. Bontempo[30], J. Y. Book Motzkin[13], C. Boscolo Meneguolo[47, c], S. Böser[40], O. Botner[61], J. Böttcher[1], J. Braun[39], B. Brinson[4], Z. Brisson-Tsavoussis[32], R. T. Burley[2], D. Butterfield[39], M. A. Campana[48], K. Carloni[13], J. Carpio[33, 34], S. Chattopadhyay[39, a], N. Chau[10], Z. Chen[55], D. Chirkin[39], S. Choi[52], B. A. Clark[18], A. Coleman[61], P. Coleman[1], G. H. Collin[14], D. A. Coloma Borja[47], A. Connolly[19, 20], J. M. Conrad[14], R. Corley[52], D. F. Cowen[59, 60], C. De Clercq[11], J. J. DeLaunay[59], D. Delgado[13], T. Delmeulle[10], S. Deng[1], P. Desiati[39], K. D. de Vries[11], G. de Wasseige[36], T. DeYoung[23], J. C. Díaz-Vélez[39], S. DiKerby[23], M. Dittmer[42], A. Domi[25], L. Draper[52], L. Dueser[1], D. Durnford[24], K. Dutta[40], M. A. DuVernois[39], T. Ehrhardt[40], L. Eidenschink[26], A. Eimer[25], P. Eller[26], E. Ellinger[62], D. Elsässer[22], R. Engel[30, 31], H. Erpenbeck[39], W. Esmail[42], S. Eulig[13], J. Evans[18], P. A. Evenson[43], K. L. Fan[18], K. Fang[39], K. Farrag[15], A. R. Fazely[5], A. Fedynitch[57], N. Feigl[8], C. Finley[54], L. Fischer[63], D. Fox[59], A. Franckowiak[9], S. Fukami[63], P. Fürst[1], J. Gallagher[38], E. Ganster[1], A. Garcia[13], M. Garcia[43], G. Garg[39, a], E. Genton[13, 36], L. Gerhardt[7], A. Ghadimi[58], C. Glaser[61], T. Glüsenkamp[61], J. G. Gonzalez[43], S. Goswami[33, 34], A. Granados[23], D. Grant[12], S. J. Gray[18], S. Griffin[39], S. Griswold[51], K. M. Groth[21], D. Guevel[39], C. Günther[1], P. Gutjahr[22], C. Ha[53], C. Haack[25], A. Hallgren[61], L. Halve[1], F. Halzen[39], L. Hamacher[1], M. Ha Minh[26], M. Handt[1], K. Hanson[39], J. Hardin[14], A. A. Harnisch[23], P. Hatch[32], A. Haungs[30], J. Häußler[1], K. Helbing[62], J. Hellrung[9], B. Henke[23], L. Hennig[25], F. Henningsen[12], L. Heuermann[1], R. Hewett[17], N. Heyer[61], S. Hickford[62], A. Hidvegi[54], C. Hill[15], G. C. Hill[2], R. Hmaid[15], K. D. Hoffman[18], D. Hooper[39], S. Hori[39], K. Hoshina[39, d], M. Hostert[13], W. Hou[30], T. Huber[30], K. Hultqvist[54], K. Hymon[22, 57], A. Ishihara[15], W. Iwakiri[15], M. Jacquart[21], S. Jain[39], O. Janik[25], M. Jansson[36], M. Jeong[52], M. Jin[13], N. Kamp[13], D. Kang[30], W. Kang[48], X. Kang[48], A. Kappes[42], L. Kardum[22], T. Karg[63], M. Karl[26], A. Karle[39], A. Katil[24], M. Kauer[39], J. L. Kelley[39], M. Khanal[52], A. Khatee Zathul[39], A. Kheirandish[33, 34], H. Kimku[53], J. Kiryluk[55], C. Klein[25], S. R. Klein[6, 7], Y. Kobayashi[15], A. Kochocki[23], R. Koirala[43], H. Kolanoski[8], T. Kontrimas[26], L. Köpke[40], C. Kopper[25], D. J. Koskinen[21], P. Koundal[43], M. Kowalski[8, 63], T. Kozynets[21], N. Krieger[9], J. Krishnamoorthi[39, a], T. Krishnan[13], K. Kruiswijk[36], E. Krupczak[23], A. Kumar[63], E. Kun[9], N. Kurahashi[48], N. Lad[63], C. Lagunas Gualda[26], L. Lallement Arnaud[10], M. Lamoureux[36], M. J. Larson[18], F. Lauber[62], J. P. Lazar[36], K. Leonard DeHolton[60], A. Leszczyńska[43], J. Liao[4], C. Lin[43], Y. T. Liu[60], M. Liubarska[24], C. Love[48], L. Lu[39], F. Lucarelli[27], W. Luszczak[19, 20], Y. Lyu[6, 7], J. Madsen[39], E. Magnus[11], K. B. M. Mahn[23], Y. Makino[39], E. Manao[26], S. Mancina[47, e], A. Mand[39], I. C. Mariş[10], S. Marka[45], Z. Marka[45], L. Marten[1], I. Martinez-Soler[13], R. Maruyama[44], J. Mauro[36], F. Mayhew[23], F. McNally[37], J. V. Mead[21], K. Meagher[39], S. Mechbal[63], A. Medina[20], M. Meier[15], Y. Merckx[11], L. Merten[9], J. Mitchell[5], L. Molchany[49], T. Montaruli[27], R. W. Moore[24], Y. Morii[15], A. Mosbrugger[25], M. Moulai[39], D. Mousadi[63], E. Moyaux[36], T. Mukherjee[30], R. Naab[63], M. Nakos[39], U. Naumann[62], J. Necker[63], L. Neste[54], M. Neumann[42], H. Niederhausen[23], M. U. Nisa[23], K. Noda[15], A. Noell[1], A. Novikov[43], A. Obertacke Pollmann[15], V. O'Dell[39], A. Olivas[18], R. Orsoe[26], J. Osborn[39], E. O'Sullivan[61], V. Palusova[40], H. Pandya[43], A. Parenti[10], N. Park[32], V. Parrish[23], E. N. Paudel[58], L. Paul[49], C. Pérez de los Heros[61], T. Pernice[63], J. Peterson[39], M. Plum[49], A. Pontén[61], V. Poojyam[58], Y. Popovych[40], M. Prado Rodriguez[39], B. Pries[23], R. Procter-Murphy[18], G. T. Przybylski[7], L. Pyras[52], C. Raab[36], J. Rack-Helleis[40], N. Rad[63], M. Ravn[61], K. Rawlins[3], Z. Rechav[39], A. Rehman[43], I. Reistroffer[49], E. Resconi[26], S. Reusch[63], C. D. Rho[56], W. Rhode[22], L. Ricca[36], B. Riedel[39], A. Rifaie[62], E. J. Roberts[2], S. Robertson[6, 7], M. Rongen[25], A. Rosted[15], C. Rott[52], T. Ruhe[22], L. Ruohan[26], D. Ryckbosch[28], J. Saffer[31], D. Salazar-Gallegos[23], P. Sampathkumar[30], A. Sandrock[62], G. Sanger-Johnson[23], M. Santander[58], S. Sarkar[46], J. Savelberg[1], M. Scarnera[36], P. Schaile[26], M. Schaufel[1], H. Schieler[30], S. Schindler[25], L. Schlickmann[40], B. Schlüter[42], F. Schlüter[10], N. Schmeisser[62], T. Schmidt[18], F. G. Schröder[30, 43], L. Schumacher[25], S. Schwirn[1], S. Sclafani[18], D. Seckel[43], L. Seen[39], M. Seikh[35], S. Seunarine[50], P. A. Sevle Myhr[36], R. Shah[48], S. Shefali[31], N. Shimizu[15], B. Skrzypek[6], R. Snihur[39], J. Soedingrekso[22], A. Søgaard[21], D. Soldin[52], P. Soldin[1], G. Sommani[9], C. Spannfellner[26], G. M. Spiczak[50], C. Spiering[63], J. Stachurska[28], M. Stamatikos[20], T. Stanev[43], T. Stezelberger[7], T. Stürwald[62], T. Stuttard[21], G. W. Sullivan[18], I. Taboada[4], S. Ter-Antonyan[5], A. Terliuk[26], A. Thakuri[49], M. Thiesmeyer[39], W. G. Thompson[13], J. Thwaites[39], S. Tilav[43], K. Tollefson[23], S. Toscano[10], D. Tosi[39], A. Trettin[63], A. K. Upadhyay[39, a], K. Upshaw[5], A. Vaidyanathan[41], N. Valtonen-Mattila[9, 61], J. Valverde[41], J. Vandenbroucke[39], T. van Eeden[63], N. van Eijndhoven[11], L. van Rootselaar[22], J. van Santen[63], F. J. Vara Carbonell[42], F. Varsi[31], M. Venugopal[30], M. Vereecken[36], S. Vergara Carrasco[17], S. Verpoest[43], D. Veske[45], A. Vijai[18], J. Villarreal[14], C. Walck[54], A. Wang[4], E. Warrick[58], C. Weaver[23], P. Weigel[14], A. Weindl[30], J. Weldert[40], A. Y. Wen[13], C. Wendt[39], J. Werthebach[22], M. Weyrauch[30], N. Whitehorn[23], C. H. Wiebusch[1], D. R. Williams[58], L. Witthaus[22], M. Wolf[26], G. Wrede[25], X. W. Xu[5], J. P. Yañez[24], Y. Yao[39], E. Yildizci[39], S. Yoshida[15], R. Young[35], F. Yu[13], S. Yu[52], T. Yuan[39], A. Zegarelli[9], S. Zhang[23], Z. Zhang[55], P. Zhelnin[13], P. Zilberman[39]

[1] III. Physikalisches Institut, RWTH Aachen University, D-52056 Aachen, Germany
[2] Department of Physics, University of Adelaide, Adelaide, 5005, Australia
[3] Dept. of Physics and Astronomy, University of Alaska Anchorage, 3211 Providence Dr., Anchorage, AK 99508, USA
[4] School of Physics and Center for Relativistic Astrophysics, Georgia Institute of Technology, Atlanta, GA 30332, USA
[5] Dept. of Physics, Southern University, Baton Rouge, LA 70813, USA
[6] Dept. of Physics, University of California, Berkeley, CA 94720, USA
[7] Lawrence Berkeley National Laboratory, Berkeley, CA 94720, USA
[8] Institut für Physik, Humboldt-Universität zu Berlin, D-12489 Berlin, Germany
[9] Fakultät für Physik & Astronomie, Ruhr-Universität Bochum, D-44780 Bochum, Germany
[10] Université Libre de Bruxelles, Science Faculty CP230, B-1050 Brussels, Belgium

PoS(ICRC2025)1181

[11] Vrije Universiteit Brussel (VUB), Dienst ELEM, B-1050 Brussels, Belgium
[12] Dept. of Physics, Simon Fraser University, Burnaby, BC V5A 1S6, Canada
[13] Department of Physics and Laboratory for Particle Physics and Cosmology, Harvard University, Cambridge, MA 02138, USA
[14] Dept. of Physics, Massachusetts Institute of Technology, Cambridge, MA 02139, USA
[15] Dept. of Physics and The International Center for Hadron Astrophysics, Chiba University, Chiba 263-8522, Japan
[16] Department of Physics, Loyola University Chicago, Chicago, IL 60660, USA
[17] Dept. of Physics and Astronomy, University of Canterbury, Private Bag 4800, Christchurch, New Zealand
[18] Dept. of Physics, University of Maryland, College Park, MD 20742, USA
[19] Dept. of Astronomy, Ohio State University, Columbus, OH 43210, USA
[20] Dept. of Physics and Center for Cosmology and Astro-Particle Physics, Ohio State University, Columbus, OH 43210, USA
[21] Niels Bohr Institute, University of Copenhagen, DK-2100 Copenhagen, Denmark
[22] Dept. of Physics, TU Dortmund University, D-44221 Dortmund, Germany
[23] Dept. of Physics and Astronomy, Michigan State University, East Lansing, MI 48824, USA
[24] Dept. of Physics, University of Alberta, Edmonton, Alberta, T6G 2E1, Canada
[25] Erlangen Centre for Astroparticle Physics, Friedrich-Alexander-Universität Erlangen-Nürnberg, D-91058 Erlangen, Germany
[26] Physik-department, Technische Universität München, D-85748 Garching, Germany
[27] Département de physique nucléaire et corpusculaire, Université de Genève, CH-1211 Genève, Switzerland
[28] Dept. of Physics and Astronomy, University of Gent, B-9000 Gent, Belgium
[29] Dept. of Physics and Astronomy, University of California, Irvine, CA 92697, USA
[30] Karlsruhe Institute of Technology, Institute for Astroparticle Physics, D-76021 Karlsruhe, Germany
[31] Karlsruhe Institute of Technology, Institute of Experimental Particle Physics, D-76021 Karlsruhe, Germany
[32] Dept. of Physics, Engineering Physics, and Astronomy, Queen's University, Kingston, ON K7L 3N6, Canada
[33] Department of Physics & Astronomy, University of Nevada, Las Vegas, NV 89154, USA
[34] Nevada Center for Astrophysics, University of Nevada, Las Vegas, NV 89154, USA
[35] Dept. of Physics and Astronomy, University of Kansas, Lawrence, KS 66045, USA
[36] Centre for Cosmology, Particle Physics and Phenomenology - CP3, Université catholique de Louvain, Louvain-la-Neuve, Belgium
[37] Department of Physics, Mercer University, Macon, GA 31207-0001, USA
[38] Dept. of Astronomy, University of Wisconsin—Madison, Madison, WI 53706, USA
[39] Dept. of Physics and Wisconsin IceCube Particle Astrophysics Center, University of Wisconsin—Madison, Madison, WI 53706, USA
[40] Institute of Physics, University of Mainz, Staudinger Weg 7, D-55099 Mainz, Germany
[41] Department of Physics, Marquette University, Milwaukee, WI 53201, USA
[42] Institut für Kernphysik, Universität Münster, D-48149 Münster, Germany
[43] Bartol Research Institute and Dept. of Physics and Astronomy, University of Delaware, Newark, DE 19716, USA
[44] Dept. of Physics, Yale University, New Haven, CT 06520, USA
[45] Columbia Astrophysics and Nevis Laboratories, Columbia University, New York, NY 10027, USA
[46] Dept. of Physics, University of Oxford, Parks Road, Oxford OX1 3PU, United Kingdom
[47] Dipartimento di Fisica e Astronomia Galileo Galilei, Università Degli Studi di Padova, I-35122 Padova PD, Italy
[48] Dept. of Physics, Drexel University, 3141 Chestnut Street, Philadelphia, PA 19104, USA
[49] Physics Department, South Dakota School of Mines and Technology, Rapid City, SD 57701, USA
[50] Dept. of Physics, University of Wisconsin, River Falls, WI 54022, USA
[51] Dept. of Physics and Astronomy, University of Rochester, Rochester, NY 14627, USA
[52] Department of Physics and Astronomy, University of Utah, Salt Lake City, UT 84112, USA
[53] Dept. of Physics, Chung-Ang University, Seoul 06974, Republic of Korea
[54] Oskar Klein Centre and Dept. of Physics, Stockholm University, SE-10691 Stockholm, Sweden
[55] Dept. of Physics and Astronomy, Stony Brook University, Stony Brook, NY 11794-3800, USA
[56] Dept. of Physics, Sungkyunkwan University, Suwon 16419, Republic of Korea
[57] Institute of Physics, Academia Sinica, Taipei, 11529, Taiwan
[58] Dept. of Physics and Astronomy, University of Alabama, Tuscaloosa, AL 35487, USA
[59] Dept. of Astronomy and Astrophysics, Pennsylvania State University, University Park, PA 16802, USA
[60] Dept. of Physics, Pennsylvania State University, University Park, PA 16802, USA
[61] Dept. of Physics and Astronomy, Uppsala University, Box 516, SE-75120 Uppsala, Sweden
[62] Dept. of Physics, University of Wuppertal, D-42119 Wuppertal, Germany
[63] Deutsches Elektronen-Synchrotron DESY, Platanenallee 6, D-15738 Zeuthen, Germany
[a] also at Institute of Physics, Sachivalaya Marg, Sainik School Post, Bhubaneswar 751005, India
[b] also at Department of Space, Earth and Environment, Chalmers University of Technology, 412 96 Gothenburg, Sweden
[c] also at INFN Padova, I-35131 Padova, Italy
[d] also at Earthquake Research Institute, University of Tokyo, Bunkyo, Tokyo 113-0032, Japan
[e] now at INFN Padova, I-35131 Padova, Italy

PoS(ICRC2025)1181

Acknowledgments

The authors gratefully acknowledge the support from the following agencies and institutions: USA – U.S. National Science Foundation-Office of Polar Programs, U.S. National Science Foundation-Physics Division, U.S. National Science Foundation-EPSCoR, U.S. National Science Foundation-Office of Advanced Cyberinfrastructure, Wisconsin Alumni Research Foundation, Center for High Throughput Computing (CHTC) at the University of Wisconsin–Madison, Open Science Grid (OSG), Partnership to Advance Throughput Computing (PATh), Advanced Cyberinfrastructure Coordination Ecosystem: Services & Support (ACCESS), Frontera and Ranch computing project at the Texas Advanced Computing Center, U.S. Department of Energy-National Energy Research Scientific Computing Center, Particle astrophysics research computing center at the University of Maryland, Institute for Cyber-Enabled Research at Michigan State University, Astroparticle physics computational facility at Marquette University, NVIDIA Corporation, and Google Cloud Platform; Belgium – Funds for Scientific Research (FRS-FNRS and FWO), FWO Odysseus and Big Science programmes, and Belgian Federal Science Policy Office (Belspo); Germany – Bundesministerium für Forschung, Technologie und Raumfahrt (BMFTR), Deutsche Forschungsgemeinschaft (DFG), Helmholtz Alliance for Astroparticle Physics (HAP), Initiative and Networking Fund of the Helmholtz Association, Deutsches Elektronen Synchrotron (DESY), and High Performance Computing cluster of the RWTH Aachen; Sweden – Swedish Research Council, Swedish Polar Research Secretariat, Swedish National Infrastructure for Computing (SNIC), and Knut and Alice Wallenberg Foundation; European Union – EGI Advanced Computing for research; Australia – Australian Research Council; Canada – Natural Sciences and Engineering Research Council of Canada, Calcul Québec, Compute Ontario, Canada Foundation for Innovation, WestGrid, and Digital Research Alliance of Canada; Denmark – Villum Fonden, Carlsberg Foundation, and European Commission; New Zealand – Marsden Fund; Japan – Japan Society for Promotion of Science (JSPS) and Institute for Global Prominent Research (IGPR) of Chiba University; Korea – National Research Foundation of Korea (NRF); Switzerland – Swiss National Science Foundation (SNSF).

PoS(ICRC2025)1181